translational velocity had no significant effect on these variables. In contrast, faster turns were accomplished by banking the wings and the body (Fig. 5e-h) farther into the turn. As a result, relative wing bank angle remained consistent across the turning treatments, just as it did between hovering and the arcing treatment with highest angular velocity and centripetal force (Fig. 4). *P*-values for these kinematic parameters can be found in Table 3.

Discussion

Whereas numerous changes in wingbeat kinematics were observed between hovering and turning, wing bank angle is a key parameter for resolving the mechanism through which flying animals orient aerodynamic force into a turn. Force vectoring is indicated by maintaining the relative wing bank angle in the same direction as acceleration and has been demonstrated in numerous studies of transient maneuvers in insects [12,33] and birds [13,21]. In our study, hummingbirds performed arced turns by banking their stroke plane (wing bank angle) into the turn for all four turning treatments. They also banked their body (body angle frontal) into the turns and maintained the position of the stroke plane relative to the body (the relative wing bank angle) for hovering and all four turning treatments. The consistency in relative wing bank angle across our treatments supports the hypothesis that hummingbirds accomplish arced turns via force vectoring and joins a recent study of pigeons [22] in expanding force vectoring to include sustained maneuvers.

An alternative hypothesis to force vectoring is that flying animals can orient aerodynamic force using left-right asymmetries in wingbeat kinematics without changing body position. Our

results show several wingstroke asymmetries during arced turns with a higher and flatter outer wing tip path and a lower, more scooped inner wing tip path, relative to each other and to hovering. However, the presence of these asymmetries alone does not preclude force vectoring from being a mechanism hummingbirds implement to orient aerodynamic force into a turn. Indeed, recent studies of pigeons [22] observed that force vectoring is modulated by wing stroke asymmetries. Intriguingly, several of the asymmetries that were not found to effect force vectoring in pigeons, such as angle of attack, stroke amplitude, and wingbeat timing, were observed in our study. The changes in wing elevation and elevation amplitude found in our study were also seen in a study of fruit flies [15] where the wing bank angle did not fully correspond to the direction of motion. This emphasizes the difficulty in resolving the function of wingbeat asymmetries from examining a single maneuver.

By comparing kinematic changes across several turns, our study identifies the function of several wingbeat asymmetries. In addition, it answers the question of whether force vectoring or sustained kinematic asymmetries are used separately or in combination to meet the challenges imposed by changes in translational velocity and turning radius. Unlike all previous studies of detailed wingbeat kinematics during maneuvering flight, ours is the first to use a balanced treatment design, which allows for independently testing the influence of radius and translational velocity. The mixed model analysis revealed that three features of asymmetrical wingbeat kinematics (elevation amplitude, stroke plane angle, and angle of attack) were associated with changes in turn radius, and two body kinematic variables (body angle frontal and wing bank angle) that control force vectoring were associated with changes in translational velocity. These kinematics were associated with changes in turning radius or translational velocity, but none were influenced by both aspects of a turn and there was no interaction between turning radius or

translational velocity for any of our ANOVAs (Table 3). This analysis suggests that wingbeat asymmetries are used to compensate for changes in turning radius and force vectoring is used to compensate for changes in velocity. Thus, rather than force vectoring and wingbeat asymmetries being mutually exclusive hypotheses, our results indicate that the two mechanisms are used simultaneously and independently to meet different aerodynamic challenges of turns.

The coordinated changes in average wing elevation, elevation amplitude, and wing rotation timing during arced turns were previously observed during yaw turns [14], which raises the question of how can a similar kinematic pattern be used to generate different motions? One potentially important wingbeat kinematic that has varied among these maneuvers is the stroke plane angle, which is a two-dimensional representation that is relative to the horizontal plane. In hovering flight, the stroke plane angle is pitched down 7-11° in both wings, such that supination is lower than pronation. During yaw turns [14] and arced turns, the stroke plane of the elevated wing is statistically indistinguishable from hovering and the stroke plane of the lowered wing is pitched up, relative to hovering. While the stroke plane angle of the lowered wing is essentially horizontal during a yaw turn, it is pitched up even farther during the upstroke of an arced turn, such that it is higher at supination than during pronation. This pattern suggests that stroke plane modulation may be an important mechanism for orienting aerodynamic forces in maneuvers with left-right differences in wing elevation. In addition, further study of other sustained maneuvers employing similar asymmetries may demonstrate that stroke plane angle is critical for orienting aerodynamic force laterally.

Tables and Figures

Figure 1. Filming apparatus

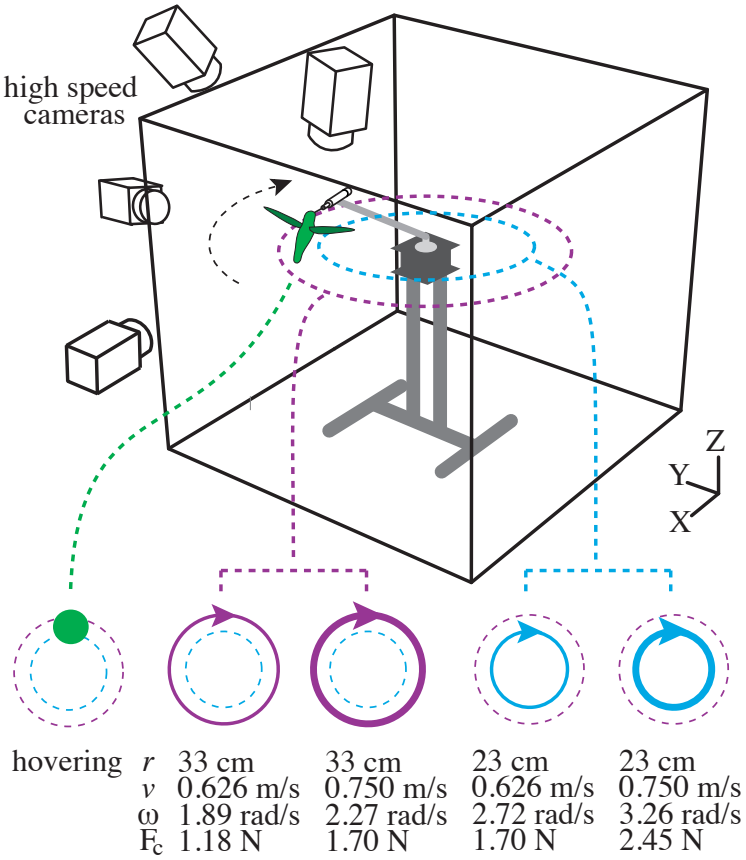

Hummingbirds fed from a 10 ml syringe while hovering and turning within an acrylic chamber. The radius and translational velocity of turns varied by adjusting the length of the feeder arm and the speed of the stepper motor's rotation. Experimental treatments and their respective turning radii (*r)*, translational velocities (*v*), angular velocities (ω), and centripetal forces (F_c) are

provided and represented by five symbols. Four high-speed cameras provided dorsal, posterior, and lateral views of hummingbirds.

Figure 2. Instantaneous wing measures

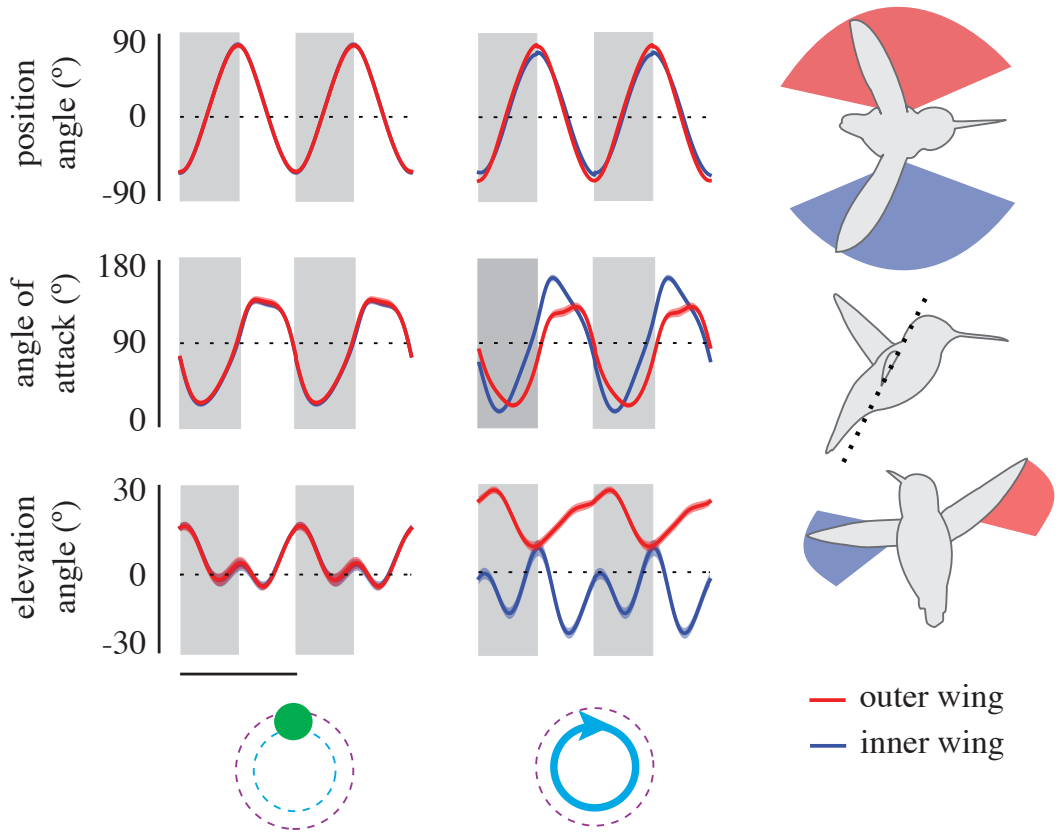

Kinematics averaged across all individuals are presented for two wingbeats of hovering (left column) and the turn with the highest centripetal force (middle column). The right column depicts position angle (top), angle of attack (middle), and elevation angle (bottom). The left wing is given in red and the right wing is in blue. Lines indicate average values and transparent bands are the standard error of the mean. Downstroke is shaded in gray. Scale bars are representative of 25 milliseconds for all graphs in this panel.

Figure 3. Analysis of kinematics between hovering and turning

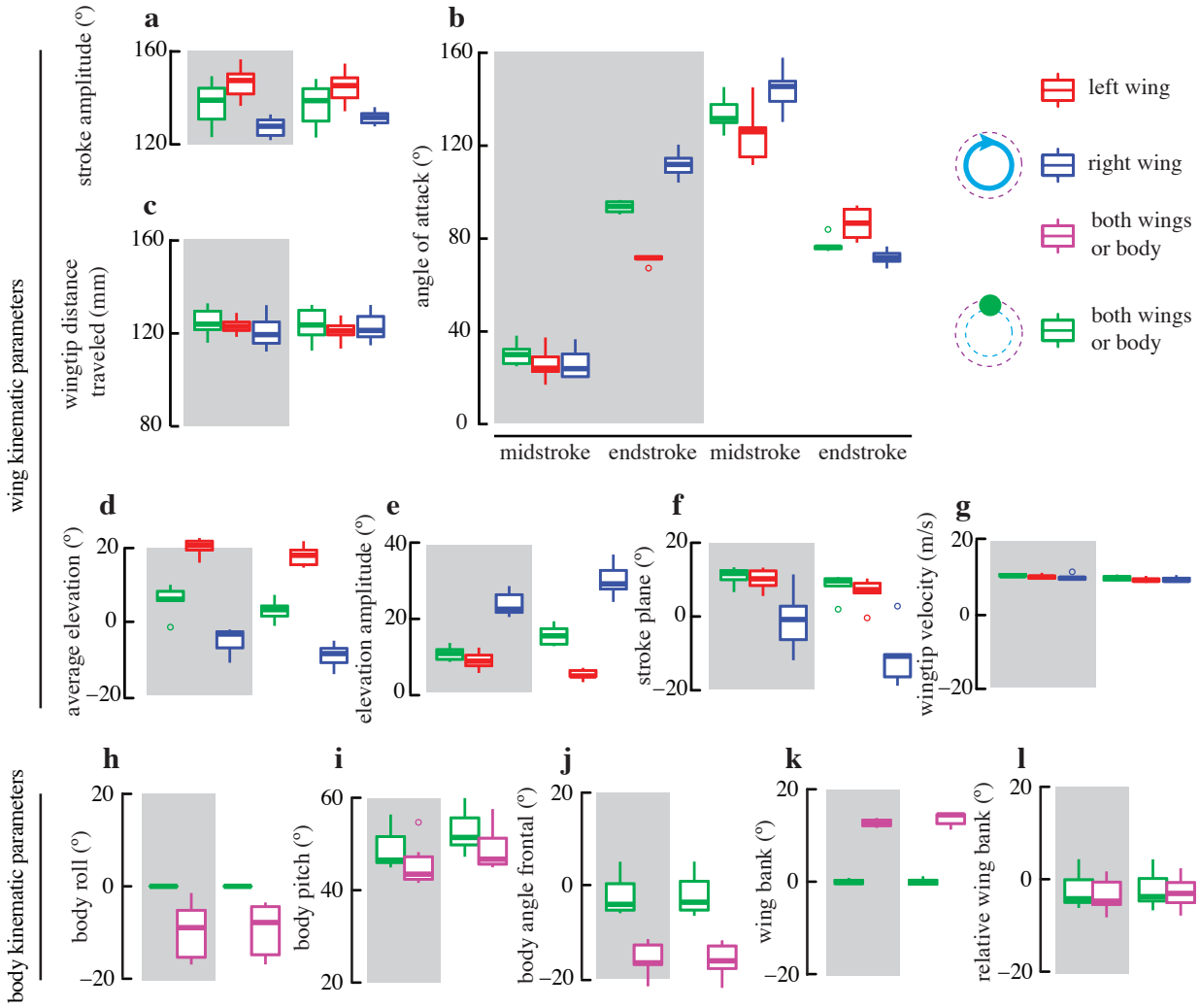

Kinematic parameters describing hovering are shown in green. Box plots from parameters related to the left and right wings of the turning treatment with the highest centripetal force are presented in red and blue, respectively. Parameters related to the body or both wings are shown in purple for turning. Downstroke is shaded in gray.

Figure 4. Average wing kinematics

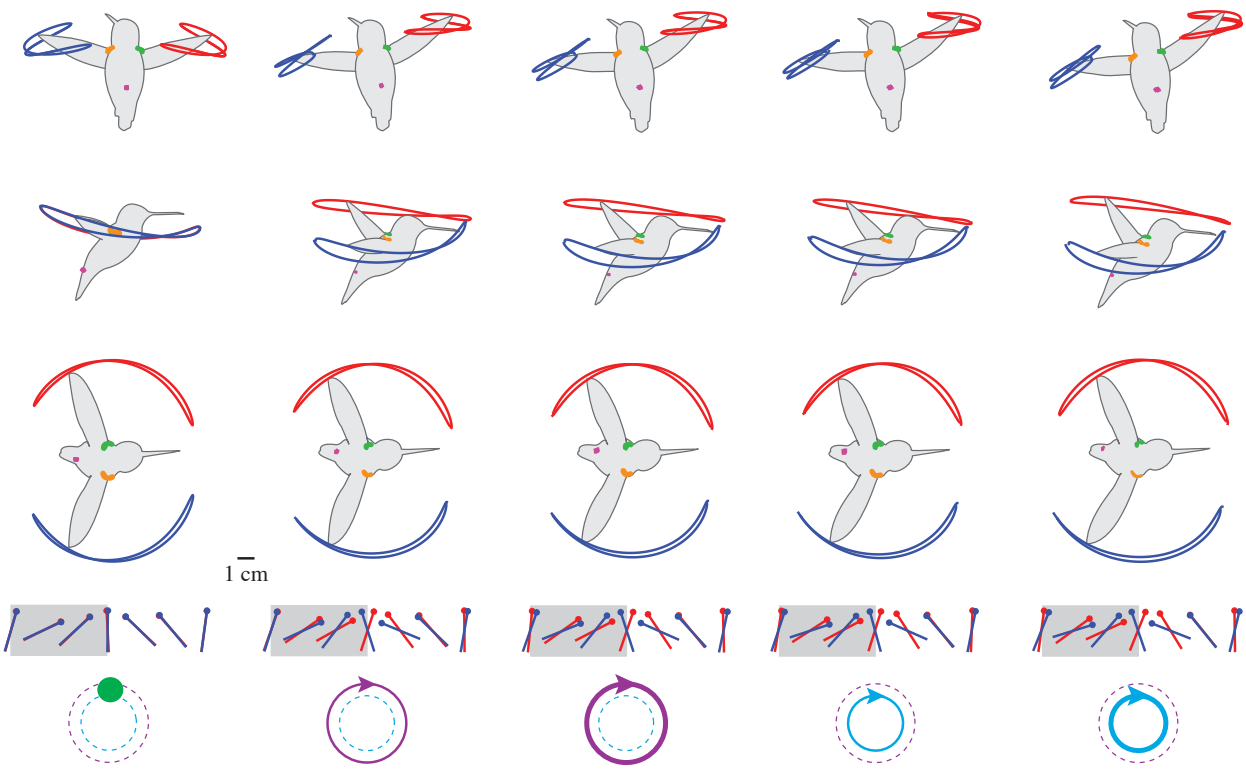

Hovering kinematics are presented in the left column and turning kinematics are arranged in order of increasing angular velocity from left to right. Anterior, lateral, and superior views are provided in the first, second, and third rows, respectively. The left wingtip path is given in red and the right wingtip is in blue. The left shoulder is given in orange and the right shoulder is given in green. The rump is given in purple. The fourth row presents the angle of attack at seven points in the wingstroke with the downstroke shaded in gray. Circles represent the leading edge of the wing.

Figure 5. Kinematic changes across turning treatments

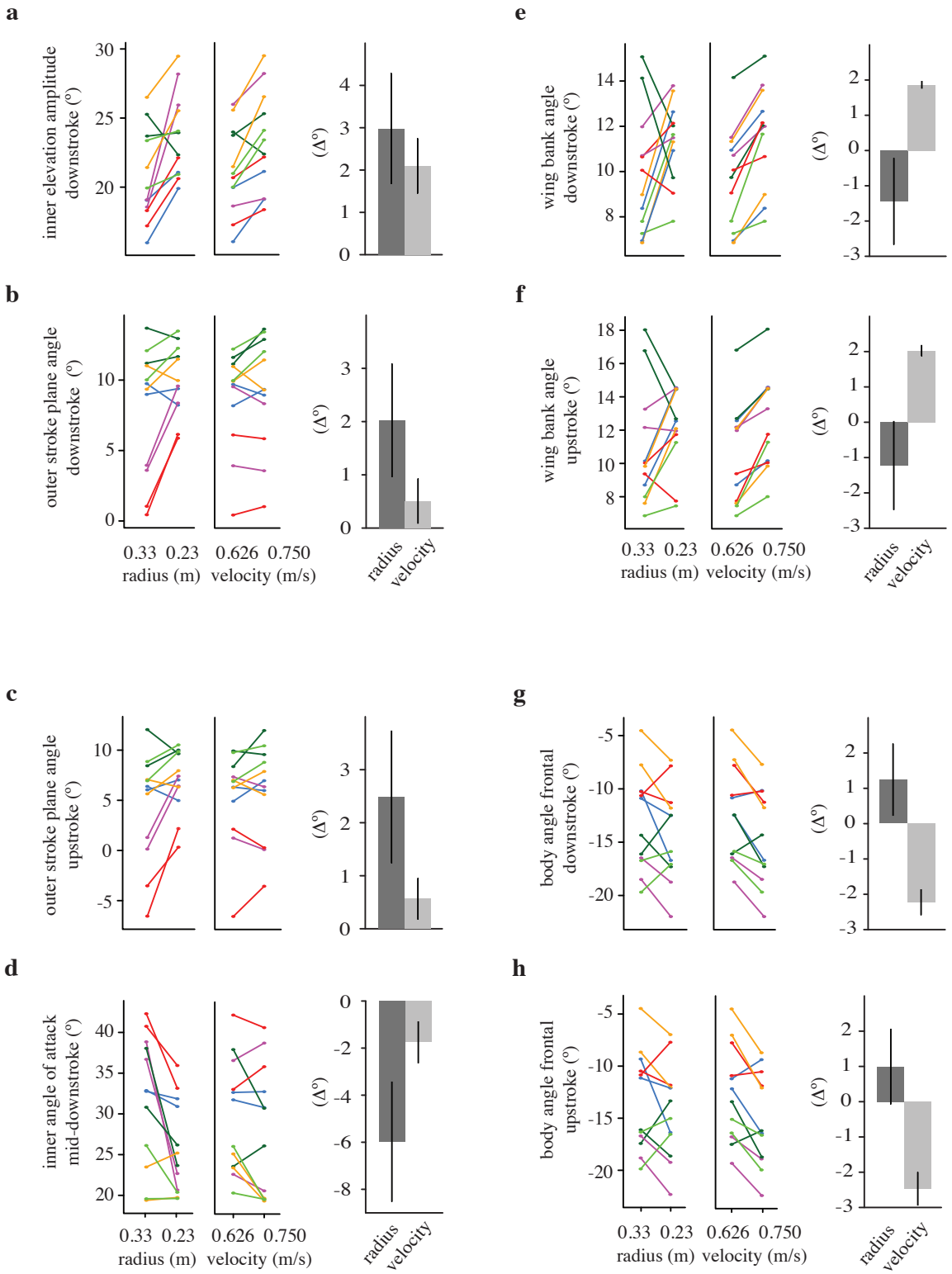

Kinematic parameters that are significantly influenced by turning radius (sub-figure a-d) and velocity (sub-figure e-h) are presented on the left and right, respectively. Plots showing the influence of radius and velocity are shown on the left and middle of each sub-figure. Averages for each level of radius or velocity are presented for each bird and are connected across changes in radius or velocity by lines. Bar plots indicating the average change in degrees across all individuals are presented with the standard error of the mean in the right plot for each kinematic.

Table 1. Mixed model ANOVA between the wing kinematics of hovering and turning

Means are presented with *P*-values from the mixed model for stroke plane angle (β), average elevation angle ($\overline{\theta}_{GR}$), stroke amplitude (Φ_{SP}), elevation amplitude (Θ_{SP}), wingtip distance traveled (WDT), average wingtip speed ($\overline{U}_{tip}$), and geometric angle of attack at mid-stroke (α_{mid}) and end-stroke (α_{end}) during upstroke ($_{US}$) and downstroke ($_{DS}$) while hovering (h) and turning (0.23 m, 0.750 m/s) for the left (l) and right (r) wings. Flight mode (hovering and turning) is the fixed effect and the random effect is bird. The degrees of freedom for all ANOVAs are 2, 10. Three post-hoc comparisons tested for significant differences between the left wing and hovering, the right wing and hovering, and the left and right wings when the overall model was significant (α=0.05). Significant *P*-values are presented in bold.

	$\bar{x}$			*P* value			
	l	h	r	overall model	l-h	r-h	l-r
β_{US} (º)	6.9	8.6	-10.8	3.76E-06	0.681	**<1.0E-04**	**<1.0E-04**

	$\bar{x}$			*P* value			
	l	h	r	overall model	l-h	r-h	l-r
β_{DS} (º)	10.2	11.1	-0.8	4.47E-04	0.914	**1.07E-07**	**1.35E-06**
$\overline{\theta}_{GR,US}$ (º)	17.9	3.1	-9.2	2.15E-09	**<2.0E-16**	**<2.0E-16**	**<2.0E-16**
$\overline{\theta}_{GR,DS}$ (º)	20.2	5.9	-5.1	4.90E-10	**<2.0E-16**	**<2.0E-16**	**<2.0E-16**
$\Phi_{SP,US}$ (º)	144.6	136.9	131.5	2.31E-03	**1.23E-02**	0.113	**3.18E-06**
$\Phi_{SP,DS}$ (º)	146.5	137.4	127.4	9.28E-05	**1.33E-03**	**3.90E-04**	**3.67E-13**
$\Theta_{SP,US}$ (º)	5.5	16.1	31.1	2.99E-07	**4.12E-08**	**1.78E-15**	**<2.0E-16**
$\Theta_{SP,DS}$ (º)	9.3	11.2	24.6	3.37E-06	0.441	**<1.0E-04**	**<1.0E-04**
WDT_{US} (mm)	120.5	123.2	122.3	0.706	-	-	-
WDT_{DS} (mm)	122.8	124.4	120.3	0.455	-	-	-
$\overline{U}_{tip,US}$ (m/s)	9.8	10.2	9.9	0.159	-	-	-
$\overline{U}_{tip,DS}$ (m/s)	10.6	10.9	10.4	0.158	-	-	-
$\alpha_{mid,US}$	124.2	133.1	143.5	1.74E-03	5.14E-02	**1.76E-02**	**1.09E-06**
$\alpha_{mid,DS}$	25.4	29.7	25.5	0.257	-	-	-
$\alpha_{end,US}$	85.1	76.7	71.3	4.07E-04	**4.00E-04**	6.38E-02	**2.37E-09**
$\alpha_{end,DS}$	70.6	93.1	111.3	4.29E-09	**<2.0E-16**	**<2.0E-16**	**<2.0E-16**

Table 2. Mixed model ANOVA between the whole body kinematics of hovering and turning

Means are presented with *P*-values from the mixed models for body pitch angle ($\chi_{GR,XZ}$), body angle frontal ($\chi_{GR,YZ}$), body roll angle ($\chi_{SP,XZ}$), relative wing bank angle (RWBA), and wing bank angle (WBA) during upstroke ($_{US}$) and downstroke ($_{DS}$) in hovering and turning (0.23 m, 0.750 m/s). Flight mode (hovering and turning) is the fixed effect and individual is the random effect. The degrees of freedom for all ANOVAs are 1, 5. Significant *P*-values are presented in bold.

	$\bar{x}$		*P* value
	hover	turning	
$\chi_{GR,XZ,US}$ (º)	52.7	48.9	0.059
$\chi_{GR,XZ,DS}$ (º)	48.8	45.6	0.069
$\chi_{GR,YZ,US}$ (º)	-2.2	-16.3	**8.00E-06**
$\chi_{GR,YZ,DS}$ (º)	-2.3	-16.1	**2.14E-05**
$\chi_{SP,XZ,US}$ (º)	2.22E-11	-9.4	**0.012**
$\chi_{SP,XZ,DS}$ (º)	-3.33E-11	-9.6	**0.014**
$RWBA_{US}$ (º)	-2.2	-2.8	0.423
$RWBA_{DS}$ (º)	-2.3	-3.4	0.162
WBA_{US} (º)	-0.018	13.5	**4.98E-06**
WBA_{DS} (º)	-0.021	12.7	**6.36E-07**

Table 3. Two-way mixed model ANOVA of whole body and wing kinematics among turning treatments

Means are presented with *P*-values from the two-way mixed model ANOVA for body pitch angle ($\chi_{GR,XZ}$), body angle frontal ($\chi_{GR,YZ}$), body roll angle ($\chi_{SP,XZ}$), relative wing bank angle (RWBA), wing bank angle (WBA), stroke amplitude (Φ_{SP}), stroke plane angle (β), elevation amplitude (Θ_{SP}), average elevation angle ($\overline{\theta}_{GR}$), average wingtip speed ($\overline{U}_{tip}$), wingtip distance travelled (WDT), and geometric angle of attack at mid-stroke (α_{mid}) and end-stroke (α_{end}) for the left ($_L$) and right ($_R$) wings during upstroke ($_{US}$) and downstroke ($_{DS}$) for all turning treatments. The levels of turning radius and translational velocity are the fixed effect and the random effect is bird. The degrees of freedom for all ANOVAs are 1, 15. Significant *P*-values are presented in bold.

	$\bar{x}$				*P* value		
	0.23 m 0.626 m/s	0.33 m 0.626 m/s	0.23 m 0.750 m/s	0.33 m 0.750 m/s	radius	velocity	interaction
$\chi_{GR,XZ,US}$ (º)	50.1	50.6	48.9	51.6	0.134	0.921	0.289
$\chi_{GR,XZ,US}$ (º)	46.8	47.5	45.6	48.4	0.107	0.859	0.352
$\chi_{GR,YZ,US}$ (º)	-12.4	-12.8	-16.3	-13.8	0.189	**0.008**	0.079
$\chi_{GR,YZ,DS}$ (º)	-12.5	-12.5	-16.1	-13.4	0.086	**0.007**	0.072
$\chi_{SP,XZ,US}$ (º)	-7.2	-7.6	-9.4	-6.7	0.500	0.721	0.381
$\chi_{SP,XZ,DS}$ (º)	-7.5	-8.7	-9.6	-7.1	0.732	0.899	0.377
$RWBA_{US}$ (º)	-1.7	-2.6	-2.8	-2.3	0.812	0.638	0.384
$RWBA_{DS}$ (º)	-2.4	-3.3	-3.4	-2.9	0.832	0.663	0.390
WBA_{US} (º)	10.8	10.2	13.5	11.5	0.108	**0.017**	0.343

	$\bar{x}$				*P* value		
	0.23 m 0.626 m/s	0.33 m 0.626 m/s	0.23 m 0.750 m/s	0.33 m 0.750 m/s	radius	velocity	interaction
WBA_{DS} (º)	10.1	9.3	12.7	10.5	0.061	**0.020**	0.343
$\Phi_{SP,L,US}$ (º)	140.4	140.8	144.6	144.2	0.992	0.093	0.850
$\Phi_{SP,L,DS}$ (º)	142.1	142.2	146.5	146.1	0.945	0.080	0.912
$\Phi_{SP,R,US}$ (º)	131.1	127.8	131.5	131.0	0.332	0.371	0.478
$\Phi_{SP,R,DS}$ (º)	127.8	125.8	127.4	128.7	0.872	0.550	0.421
$\beta_{L,US}$ (º)	6.8	4.1	6.9	4.9	**0.015**	0.600	0.715
$\beta_{L,DS}$ (º)	9.6	7.8	10.2	8.1	**0.016**	0.543	0.824
$\beta_{R,US}$ (º)	-8.2	-11.1	-10.8	-10.8	0.467	0.567	0.495
$\beta_{L,DS}$ (º)	-0.7	-4.6	-0.8	-2.6	0.185	0.661	0.615
$\Theta_{SP,L,US}$ (º)	6.2	7.5	5.5	6.4	0.073	0.115	0.705
$\Theta_{SP,L,DS}$ (º)	6.7	8.4	9.3	7.8	0.910	0.268	0.100
$\Theta_{SP,R,US}$ (º)	28.7	26.6	31.1	28.2	0.047	0.098	0.726
$\Theta_{SP,R,DS}$ (º)	22.8	19.5	24.6	21.9	**0.004**	0.036	0.757
$\bar{\theta}_{GR,L,US}$ (º)	15.3	14.5	17.9	16.0	0.126	0.032	0.534
$\bar{\theta}_{GR,L,DS}$ (º)	17.2	16.9	20.2	18.2	0.239	0.031	0.372
$\bar{\theta}_{GR,R,US}$ (º)	-6.2	-5.9	-9.2	-7.0	0.204	0.040	0.323
$\bar{\theta}_{GR,R,DS}$ (º)	-2.9	-1.7	-5.1	-2.7	0.036	0.063	0.477
$\bar{U}_{tip,L,US}$ (m/s)	9.8	9.8	9.8	9.9	0.402	0.675	0.671
$\bar{U}_{tip,L,DS}$ (m/s)	10.6	10.7	10.6	10.7	0.505	0.828	0.894
$\bar{U}_{tip,R,US}$ (m/s)	10.0	9.7	9.9	9.8	0.069	0.710	0.233
$\bar{U}_{tip,R,DS}$ (m/s)	10.5	10.3	10.4	10.4	0.443	0.889	0.380
$WDT_{L,US}$	119.2	120.8	120.5	122.9	0.306	0.371	0.841

	$\bar{x}$				*P* value		
	0.23 m 0.626 m/s	0.33 m 0.626 m/s	0.23 m 0.750 m/s	0.33 m 0.750 m/s	radius	velocity	interaction
(mm)							
$WDT_{L,DS}$ (mm)	121.5	122.4	122.8	125.4	0.331	0.250	0.620
$WDT_{R,US}$ (mm)	122.2	119.1	122.3	122.2	0.393	0.394	0.406
$WDT_{R,DS}$ (mm)	120.8	117.9	120.3	122.2	0.806	0.362	0.243
$\alpha_{mid,L,US}$ (°)	125.0	128.5	124.2	125.6	0.098	0.194	0.449
$\alpha_{end,L,US}$ (°)	82.9	85.3	85.9	86.5	0.391	0.226	0.595
$\alpha_{mid,R,US}$ (°)	143.2	146.9	143.5	143.9	0.215	0.399	0.297
$\alpha_{end,R,US}$ (°)	73.4	74.5	71.3	72.7	0.331	0.135	0.891
$\alpha_{mid,L,DS}$ (°)	25.8	26.7	25.4	26.2	0.476	0.694	0.956
$\alpha_{end,L,DS}$ (°)	74.6	74.1	70.6	73.8	0.390	0.173	0.248
$\alpha_{mid,R,DS}$ (°)	26.2	33.0	25.5	30.6	**0.005**	0.423	0.644
$\alpha_{end,R,DS}$ (°)	107.7	109.7	111.3	110.5	0.797	0.360	0.555

Concluding Chapter

The research presented in this thesis identifies the methods hummingbirds use to orient aerodynamic force into a turn and describes how kinematics vary in response to changes in turning radius and velocity. Notably, hummingbirds control turning radius through wingbeat asymmetries and translational velocity through force vectoring. Both of these mechanisms have been previously described during turns in other taxa [13,15], but their combination to simultaneously control separate aspects of a single maneuver is unprecedented. This thesis compliments published literature and expands upon recent findings [22] to offer the first description of how changes in turning radius and velocity are accomplished through adjustments in kinematics. In addition to contributing to our understanding of turning mechanics, these findings are also relevant to maneuverability in a broad context by identifying a clear relationship between behavior and physical challenges.

While feeder tracking represents a powerful mechanism for studying maneuverability in hummingbirds, it suffers from some limitations. The first is that it is unknown whether the trajectories and velocities in a given study are representative of flight in natural conditions. It is possible that the average arced turn of a hummingbird has a larger turning radius or a faster translational velocity. Similarly, the range of translational velocities where the feeder elicited a sustained turn from the hummingbird was limited. For slowly revolving feeders used in preliminary research and training, hummingbirds implemented a series of maneuvers where an individual would hover while feeding and fly forward in a straight line to intercept the feeder as

it moved away from them. At high velocities, hummingbirds were incapable of consistently tracking the feeder and would accelerate and decelerate during feeding. This limited the range of velocities that could be examined with our methods and it is possible that new kinematic mechanisms may emerge at higher turning velocities. These limitations, however, are not likely to extend to changes in turning radius. Our smallest turning radius, at 0.23 m, represents a relatively tight arcing turn in the context of a hummingbird's wingspan. The average wing length of the individuals used in this study was 0.053 m (Appendix Table 4), meaning that the turning radius represented just over four wing lengths. In addition, arced turns featured marked similarities in average wing elevation, elevation amplitude, and wing rotation with yaw turns [14], where the turning radius was zero. Despite the limitations of feeder tracking, the results obtained in this study illustrate the kinematics over the range of experimental treatments and offer a set of mechanisms that can be tested at higher centripetal forces and translation velocities.

Several avenues for future research on turning mechanics are suggested by the results of this study. One potential direction would be to repeat the experimental treatments with the addition of flow visualization techniques that would identify the direction of the vortices generated by each wing [34]. Such a study could provide additional insight for the function of force vectoring and asymmetrical wing kinematics in turning. Care would have to be taken, however, to ensure that the revolving feeder did not create a wake that obscured the jets produced by each wing. A second topic that could be explored is whether there is an energetic difference between force vectoring and asymmetrical wingbeats. Previous studies of flight energetics and thermogenesis in hummingbirds [35,36] have established methods for measuring oxygen consumption in hummingbirds and similar methods could be used to determine the energetic costs of each mechanism of lateral force production. A third question that could be

addressed is how arced turns are initiated and concluded in hummingbirds and whether these transitional periods are affected by a turn's radius or translational velocity. To answer this question, flight corridors similar to those used in other turning studies [13,21,22] could be constructed that would require different turning radii. A feeder could then travel down these corridors at specified speeds. High-speed cameras would record the kinematic transition from forward flight to turning and from turning to forward flight. Lastly, another potential area of research is diving, which is related to turning. Instead of requiring lateral force to conduct an arcing turn, a dive would require vertical force to counteract gravity and provide centripetal force. A similar apparatus to the one used in this study could incorporate a feeder that revolved perpendicular to the horizon. This experiment could detail the wing kinematics required to execute a dive and explain how the kinematics change with variations in dive radius, velocity, and centripetal force. While the limitations of feeder tracking would likely preclude recording the accelerations observed during free flight [18], such a study could provide valuable insights into how dives are initiated, controlled, and concluded.

Our results demonstrate that hummingbirds control turning radius and velocity by adjusting left-right wingbeat kinematics and body and wing bank angle, respectively. However, it is unknown if other flying animals control these aspects of a turn in a similar manner. Because previous studies of turning have not varied turning radius or velocity, it is unknown how these aspects of a turn are controlled by body and wing kinematics. Many species of insects, birds, and bats have a more vertically oriented wingstroke, and they may alter different aspects of their wingbeat kinematics to modulate turning radius in particular. One challenge posed by studying turning in other taxa is that it can be difficult to train individuals to follow defined trajectories and speeds. To resolve this issue within insects, similar methods to previous studies [15,33]

could record a large number of turns and those meeting specific criteria for turning radius and velocity could be selected for kinematic analysis. Among other bird species, individuals could be trained to fly at two velocities through multiple flight corridors that are similar to those used in previous studies [13,21,22] but would require different turning radii. A recent study of turning pigeons [22] found several wingstroke asymmetries, and it is possible that these asymmetries are important in modulating turn radius in addition to initiating turns and controlling force vectoring. Similar experimental treatments could also prove informative for studies of bat flight. A previous study of bats [37] determined that bats rotated their bodies into a turn without changing trajectory during upstroke and used force vectoring to orient force into a turn during downstroke. Comparing different turns within bats could provide insight into the role the upstroke and downstroke have in controlling turning radius and speed. These studies would provide valuable insight into how body and wingstroke orientation influence turning mechanics and offer opportunities to further explore how turns are accomplished during flapping flight.

References

1. Dudley, R. & Yanoviak, S. P. 2011 Animal Aloft: The Origins of Aerial Behavior and Flight. *Integr. Comp. Biol.* **51**, 926–936. (doi:10.1093/icb/icr002)

2. Yanoviak, S. P., Munk, Y. & Dudley, R. 2011 Evolution and Ecology of Directed Aerial Descent in Arboreal Ants. *Integr. Comp. Biol.* **51**, 944–956. (doi:10.1093/icb/icr006)

3. Emerson, S. B. & Koehl, M. A. R. 1990 The Interaction of Behavioral and Morphological Change in the Evolution of a Novel Locomotor Type: 'Flying' Frogs. *Evolution* **44**, 1931. (doi:10.2307/2409604)

4. Altshuler, D. L. 2006 Flight performance and competitive displacement of hummingbirds across elevational gradients. *Am. Nat.* **167**, 216–229.

5. Combes, S. A., Rundle, D. E., Iwasaki, J. M. & Crall, J. D. 2012 Linking biomechanics and ecology through predator-prey interactions: flight performance of dragonflies and their prey. *J. Exp. Biol.* **215**, 903–913. (doi:10.1242/jeb.059394)

6. Dudley, R. 2002 Mechanisms and implications of animal flight maneuverability. *Integr. Comp. Biol.* **42**, 135–140.

7. Aldridge, H. D. 1986 Kinematics and aerodynamics of the greater horseshoe bat, Rhinolophus ferrumequinum, in horizontal flight at various flight speeds. *J. Exp. Biol.* **126**, 479–497.

8. Wang, H., Zeng, L., Liu, H. & Yin, C. 2003 Measuring wing kinematics, flight trajectory and body attitude during forward flight and turning maneuvers in dragonflies. *J. Exp. Biol.* **206**, 745–757. (doi:10.1242/jeb.00183)

9. Shelton, R. M., Jackson, B. E. & Hedrick, T. L. 2014 The mechanics and behavior of Cliff Swallows during tandem flights. *J. Exp. Biol.* (doi:10.1242/jeb.101329)

10. Alexander, D. E. 1986 Wind tunnel studies of turns by flying dragonflies. *J. Exp. Biol.* **122**, 81–98.

11. Pennycuick, C. J. 1975 Avian Biology. In *Mechanics of Flight* (eds D. Farner & J. King), New York, N.Y.: Academic Press.

12. Muijres, F. T., Elzinga, M. J., Melis, J. M. & Dickinson, M. H. 2014 Flies Evade Looming Targets by Executing Rapid Visually Directed Banked Turns. *Science* **344**, 172–177. (doi:10.1126/science.1248955)

13. Ros, I. G., Bassman, L. C., Badger, M. A., Pierson, A. N. & Biewener, A. A. 2011 Pigeons steer like helicopters and generate down- and upstroke lift during low speed turns. *Proc. Natl. Acad. Sci.* **108**, 19990–19995. (doi:10.1073/pnas.1107519108)

14. Altshuler, D. L., Quicazan-Rubio, E. M., Segre, P. S. & Middleton, K. M. 2012 Wingbeat kinematics and motor control of yaw turns in Anna's hummingbirds (Calypte anna). *J. Exp. Biol.* **215**, 4070–4084. (doi:10.1242/jeb.075044)

15. Bergou, A. J., Ristroph, L., Guckenheimer, J., Cohen, I. & Wang, Z. J. 2010 Fruit Flies Modulate Passive Wing Pitching to Generate In-Flight Turns. *Phys. Rev. Lett.* **104**. (doi:10.1103/PhysRevLett.104.148101)

16. Warrick, D. R., Hedrick, T. L., Fernández, M. J., Tobalske, B. W. & Biewener, A. A. In press. Hummingbird Flight.

17. Stolpe, M. & Zimmer, K. 1939 Der schwirrflug des kolibri im zeitlupenfilm. *J. Ornithol.* **87**, 136–155.

18. Clark, C. J. 2009 Courtship dives of Anna's hummingbird offer insights into flight performance limits. *Proc. R. Soc. B Biol. Sci.* **276**, 3047–3052. (doi:10.1098/rspb.2009.0508)

19. Tobalske, B. W., Warrick, D. R., Clark, C. J., Powers, D. R., Hedrick, T. L., Hyder, G. A. & Biewener, A. A. 2007 Three-dimensional kinematics of hummingbird flight. *J. Exp. Biol.* **210**, 2368–2382. (doi:10.1242/jeb.005686)

20. Sapir, N. & Dudley, R. 2012 Backward flight in hummingbirds employs unique kinematic adjustments and entails low metabolic cost. *J. Exp. Biol.* **215**, 3603–3611. (doi:10.1242/jeb.073114)

21. Hedrick, T. L. & Biewener, A. A. 2007 Low speed maneuvering flight of the rose-breasted cockatoo (Eolophus roseicapillus). I. Kinematic and neuromuscular control of turning. *J. Exp. Biol.* **210**, 1897–1911. (doi:10.1242/jeb.002055)

22. Ros, I. G., Badger, M. A., Pierson, A. N., Bassman, L. C. & Biewener, A. A. 2015 Pigeons produce aerodynamic torques through changes in wing trajectory during low speed aerial turns. *J. Exp. Biol.* **218**, 480–490. (doi:10.1242/jeb.104141)

23. Russell, S. M. & Russell, R. O. 2001 The North American Banders'manual for Banding.

24. Hedrick, T. L. 2008 Software techniques for two- and three-dimensional kinematic measurements of biological and biomimetic systems. *Bioinspir. Biomim.* **3**, 034001. (doi:10.1088/1748-3182/3/3/034001)

25. Pinheiro, J., Bates, D., DebRoy, S., Sarkar, D. & R Core Team 2015 *nlme: Linear and Nonlinear Mixed Effects Models*.

26. Pinheiro, J. & Bates, D. 2000 *Mixed-Effects Models in S and S-PLUS*. New York, N.Y.: Springer.

27. R Core Team 2014 *R: A language and environment for statistical computing*. Vienna, Austria: R Foundation for Statistical Computing.

28. Bretz, F., Hothorn, T. & Westfall, P. 2011 *Multiple Comparisons Using R*. Boca Raton, FL: CRC Press.

29. Curran-Everett, D. 2000 Multiple comparisons: philosophies and illustrations. *Am. J. Physiol.-Regul. Integr. Comp. Physiol.* **279**, R1–R8.

30. Storey, J. D. 2002 A direct approach to false discovery rates. *J. R. Stat. Soc. Ser. B Stat. Methodol.* **64**, 479–498.

31. Storey, J. D. & Tibshirani, R. 2003 Statistical significance for genomewide studies. *Proc. Natl. Acad. Sci.* **100**, 9440–9445.

32. Dabney, A. & Storey, J. D. In press. *qvalue: Q-value estimation for false discovery rate control*.

33. Fry, S., Sayaman, R. & Dickinson, M. H. 2003 The Aerodynamics of Free-Flight Maneuvers in Drosophila. *Science* **300**, 495–498.

34. Pournazeri, S., Segre, P. S., Princevac, M. & Altshuler, D. L. 2012 Hummingbirds generate bilateral vortex loops during hovering: evidence from flow visualization. *Exp. Fluids* **54**. (doi:10.1007/s00348-012-1439-5)

35. Chai, P. & Dudley, R. 1996 Limits to flight energetics of hummingbirds hovering in hypodense and hypoxic gas mixtures. *J. Exp. Biol.* **199**, 2285–2295.

36. Chai, P. 1998 Flight thermogenesis and energy conservation in hovering hummingbirds. *J. Exp. Biol.* **201**, 963–968.

37. Iriarte-Diaz, J. & Swartz, S. M. 2008 Kinematics of slow turn maneuvering in the fruit bat Cynopterus brachyotis. *J. Exp. Biol.* **211**, 3478–3489. (doi:10.1242/jeb.017590)

Appendices

Table 4. Bird morphometrics

average body mass (M), wing length (R), wing area (S), aspect ratio (AR), and the non-dimensional radii of the first [$\hat{r}_1(S)$], second [$\hat{r}_2(S)$], and third [$\hat{r}_3(S)$] moments of wing area for each bird.

bird	M (g)	R (mm)	S (mm^2)	AR	$\hat{r}_1(S)$	$\hat{r}_2(S)$	$\hat{r}_3(S)$
1	4.26	55.445	1620.070	7.593	0.423	0.496	0.549
2	4.38	54.228	1653.012	7.130	0.447	0.521	0.573
3	4.15	52.549	1518.295	7.278	0.433	0.507	0.561
4	4.56	53.641	1524.945	7.557	0.434	0.506	0.558
5	4.09	52.132	1483.544	7.345	0.420	0.495	0.549
6	4.48	53.521	1559.219	7.366	0.430	0.506	0.560

Body mass is averaged across trials. Wing measurements are an average of both wings, with the exception of non-dimensional radii of wing area, which were calculated from a digital photograph of a single wing.